COMPARTIVE STUDY OF DAMAGE-SENSITIVE INDEXES USED FOR STRUCTURAL HEALTH MONITORING OF SMART STRUCTURES

Douglas Domingues Bueno, ddbueno@dem.feis.unesp.br
GMSINT – Grupo de Materiais e Sistemas Inteligentes, Department of Mechanical Engineering, Faculdade de Engenharia de Ilha Solteira – UNESP, Av. Brasil 56, Ilha Solteira, SP, Brazil, ZIP CODE 15385000, www.dem.feis.unesp.br/gmsint

Samuel da Silva, samsilva@fem.unicamp.br
Department of Mechanical Design, Faculty of Mechanical Engineering, State University of Campinas – UNICAMP, Rua Mendeleiev, s/n, Cidade Universitária, P.O. Box 6122, ZIP CODE 13083-970, Campinas, SP, Brazil, http://www.fem.unicamp.br/%7Esamsilva/

Clayton Rodrigo Marqui, clayton_rm@dem.feis.unesp.br
Vicente Lopes Junior, vicente@dem.feis.unesp.br
GMSINT – Grupo de Materiais e Sistemas Inteligentes, Department of Mechanical Engineering, Faculdade de Engenharia de Ilha Solteira – UNESP, Av. Brasil 56, Ilha Solteira, SP, Brazil, ZIP CODE 15385000, www.dem.feis.unesp.br/gmsint

Abstract. *This paper aims to compare different damage-sensitive indexes used to detect and locate minor structural faults within aerospace, civil and mechanical systems. Damage metrics charts are directly computed using a non-parametric relationship obtained from electrical signals of patches of piezoceramics (PZT) coupled in flexible structures, namely smart structure. Four commons damage metrics charts are investigated: the root-means-square deviation, the correlation coefficient deviation, and* H_2 *and* H_∞ *norms. This work also includes the analysis of the frequency range utilized to compute those damage indexes. Comparisons are made in an experimental test-bed using an aluminum beam with two PZTs bonded on the surface considering several structural conditions. The experimental results demonstrated the efficacy of the approach. It can be pointed out that careful attention is necessary to choose correctly the index and the range of frequencies for monitoring a real-world structure using smart structures concepts.*

Keywords*: structural health monitoring, smart structures, root-means-square and correlation coefficient deviation,* H_2 *and* H_∞ *norm.*

1. INTRODUCTION

Smart materials technology plays an important hole in modern structural projects due to economical, equipment availability and safety reasons, particularly in aircraft structures (Moura Jr. et al., 2006). A powerful approach involving smart materials technology by using mainly piezoceramics actuators/sensors has been extensively studied recently. However, it is still not developed enough to be a “plug-n-play” monitoring system due to several practical reasons discussed in Peairs et al. (2006).

The biggest problem in structural health monitoring is to decide correctly whether damage is present or not. The partitioning of the damage-sensitive feature to separate the healthy and damaged conditions is traditionally conducted in frequency-domain by different indexes, besides some exceptions, like Silva et al. (2007) who proposed an index in the time-domain. There are different proposals for using damage metric charts. Depending of the application, each index has advantages and drawbacks. However, it is not common to find out comparative studies of the performance and frequency range for different indexes applied in the same structure. An interesting study in this sense was performed by Zagrai and Giurgiutiu (2001).

Thus, this paper proposes a comparative study among four indexes used for damage detection through electrical measurements from input/output data in the frequency domain obtained by PZTs bonded in a lightweight structure. These indexes are the root-means-square deviation (RMSD), the correlation coefficient deviation, and H_2 and H_∞ norms. The last two are not commonly used in SHM, but they present suitable properties for damage detection (Gawronski and Sawicki, 2000; Bueno et al., 2006). In order to illustrate the results an experimental test-bed using a beam structure was performed. The next sections describe the procedure proposed and the reached conclusions.

2. DAMAGE-SENSITIVE INDEXES

The four indexes obtained by frequency response function investigated in this paper are briefly described below.

(a) Root-Means-Square Deviation (RMSD)

The RMSD index is presented here in the following form, (Lopes Jr. et al., 2000):

$$M = \sum_{i=1}^{n} \sqrt{\frac{\left[\operatorname{Re}(Z_{i,1}) - \operatorname{Re}(Z_{i,2})\right]^2}{\left[\operatorname{Re}(Z_{i,1})\right]^2}} \tag{1}$$

where $Z_{i,1}$ is the electrical impedance of the baseline condition, or healthy structure, of the PZT sensor and $Z_{i,2}$ is the signal in the same PZT in unknown structural conditions at frequency interval i. Only the real part of the signal is analyzed because it is more sensitive to structural modifications than the imaginary part, since they are dominated by the capacitive response of the sensor and is less sensitive to structural damage effect (Silva et al., 2007).

(b) Correlation Coefficient Deviation (CCDM):

The CCDM is closely related to the RMSD and is given by:

$$1-\rho = 1-\frac{\operatorname{cov}(Z_1, Z_2)}{S_{Z_1} S_{Z_2}} = 1-\frac{1}{n-1}\frac{\sum_{i=1}^{n}\left(Z_{i,1}-\overline{Z}_1\right)\left(Z_{i,2}-\overline{Z}_2\right)}{S_{Z_1} S_{Z_2}} \tag{2}$$

where ρ is the correlation coefficient, cov is the cross-covariance and S is relative to the sample standard deviation. Z is the real part of the signal in the frequency domain. Here ρ is the value that indicate how well the baseline (reference signal) and the measurements in the unknown conditions are linearly related. Thus, high values are expressive that the data are uncorrelated, or else, there is a variation, probably occurred due to the damage.

(c) H_2 Norm

Norms of systems are as measured of size and can be used for diverse applications. It can be point out the use for damage locations (Gawronski and Sawicki, 2000; Marqui *et al.*, 2006), reduction of models (Gawronski and Juang, 1990 and Mahmoud *et al.*, 2002), control (Mustafa and Glover, 1991 and Burl, 1999), and optimal placement of sensors and actuators (Gawronski, 1998; Panossian *et al.*, 1998 and Bueno *et al.*, 2006). The H_2 norm of a system is used to characterize the system itself, along with its modes and its sensors. Let G(ω) be a transfer function of a system. The H_2 norm of the system is defined as (Gawronski, 1998)

$$\|G\|_2^2 = \frac{1}{2\pi}\int_{-\infty}^{+\infty} \operatorname{tr}(G^*(\omega)G(\omega))d\omega \tag{3}$$

where tr is the trace of $G^*(\omega)G(\omega)$

Generally, the H_2 norm is computed using modal coordinates, but in this way is necessary to obtain a model for the equation motion. The numerical value for the H_2 norm for a SISO (single-input-single-output) system correspond the area under the frequency response function (FRF) of the system (Gawronski, 1998). In practical situations, the obtaining of the mathematical model can be difficult, so, to overcome this situation, one can consider the area of the frequency response function. In this paper, the area under of the FRF curve was computed using the Trapezoidal method, implemented in the software Matlab® through command “trapz”.

The H_2 norm can be used for damage detection following the procedure: it considers the norm computed using the j*th* PZT actuator/sensor; and denoting it for a healthy structure by $\|G_{shj}\|_2$, and j*th* PZT actuator/sensor norm of a damaged structure by $\|G_{sdj}\|_2$. The j*th* sensor index of the structural damage is defined as weighted difference between the j*th* sensor norm of a healthy and damaged structure (Gawronski and Sawicki, 2000)

$$\sigma_{sj} = \frac{\left|\|G_{shj}\|_2^2 - \|G_{sdj}\|_2^2\right|}{\|G_{shj}\|_2^2} \tag{4}$$

where j = 1,…, r; and r is the PZT actuator/sensor number. Note that the sensor index reflects the impact of the structural damage on the j*th* sensor.

(d) H_∞ Norm

The $H\infty$ norm of a stable system with a transfer function G(ω) is defined as

$$\|G\|_{\infty} = \max_{\infty} \sigma_{max}(G(\omega)) \tag{5}$$

where $\sigma_{max}(G(\omega))$ is the largest singular value of $G(\omega)$ (Maia et al., 1996).

The H_{∞} norm of a SISO system is the peak magnitude of the transfer function, in terms of its singular values. Due the independence of the modes, the H_{∞} norm of the system is the largest value of the mode norms, i.e.,

$$\|G\|_{\infty} = \max_{i} \|G_i\|_{\infty}, \quad i = 1,\ldots,n \tag{6}$$

The H_{∞} norm for damage detection was previously presented in Bueno et al. (2006), but the idea is the same proposed for the H_2 norm. It considers the norm of the *ith* mode computed using the *jth* PZT actuator/sensor; and denoting it for a healthy structure by $\|G_{shji}\|_{\infty}$, and *jth* PZT actuator/sensor norm of a damaged structure by $\|G_{sdji}\|_{\infty}$. The *jth* sensor index of the structural damage is defined as weighted difference between the sum of the *jth* sensor norm for each mode considering a healthy and damaged structure

$$\sigma_{sj} = \frac{\left| \left(\sum_{i=1}^{n} \|G_{shji}\|_{\infty} \right)^2 - \left(\sum_{i=1}^{n} \|G_{sdji}\|_{\infty} \right)^2 \right|}{\left(\sum_{i=1}^{n} \|G_{shji}\|_{\infty} \right)^2} \tag{7}$$

where j = 1,…, r; and r is the PZT actuator/sensor number. This sensor index reflects the impact of the structural damage on the *jth* sensor. For practical situations, it is possible to consider $\sum_{i=1}^{n} \|G_{shji}\|_{\infty} = \sum_{i=1}^{p} \|G_{shji}\|_{\infty}$ and $\sum_{i=1}^{n} \|G_{sdji}\|_{\infty} = \sum_{i=1}^{p} \|G_{sdji}\|_{\infty}$, where p is the number of considered modes.

3. EXPERIMENTAL TEST DESCRIPTION

This section describes the tests that were conducted in order to verify the applicability of these different methods. The experiments were done in a smart aluminum beam, shown in Fig. 1. Two PZT elements, called PZT1 and PZT2, were bonded on the beam surface. Table 1 shows the geometric properties of the PZT patches and of the beam. The input excitation was a white noise within +/- 1 V saturation limits. The schematic diagram of the measurement network with the positions of the sensing-actuating PZTs is shown in Fig. 2.

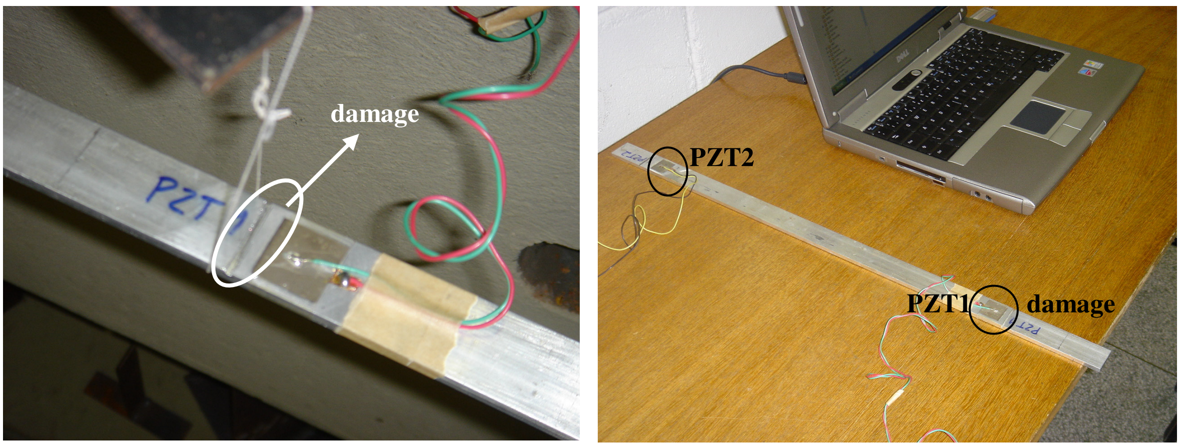

Figure 1. View of the smart beam used in the experimental tests. (a) PZT bonded in the smart beam and detail of the damage (transversal cut). (b) Smart beam with two bonded PZT patches.

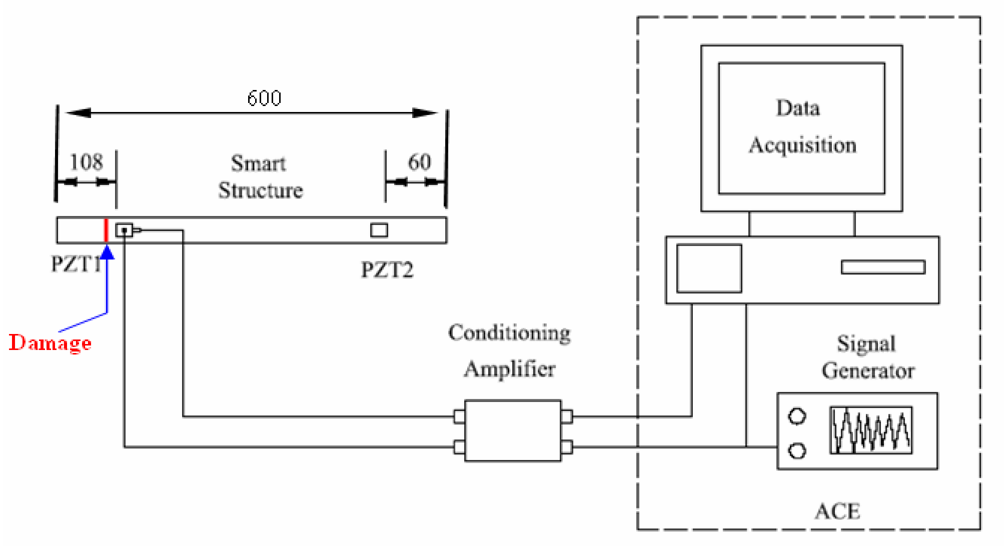

Figure 2. Schematic diagram of the measurement setup; dimensions in mm.

Table 1. Dimensions of the host structure and of the PZTs (from PSI-5A-S4, Piezo Systems®, Inc.)

Property	Beam [mm]	PZT [mm]
Length	600	20
Width	25	20
Thickness	5	0.27

The input excitation and data acquisition were led using a commercial system from Data Physics controlled by SignalCalc ACE® software. The signals were recorded in two channels in the time-domain with a sampling rate of 102.4 kHz, producing 8192 time samples each. An electrical circuit was used for conditioning and to amplifier the output voltage from each PZT patch.

The damages (simulated "crack") were introduced by a transversal cut on the surface of the beam, near to PZT1, 14 mm from the free-end of the beam, see Fig. 1. Various depths were done to represent different levels of severity. Table 2 describes the structural conditions investigated. In each condition were stored three sets of input-output data from PZT1 and PZT2. These acquisitions were performed in different moments in order to include some variability of the environment into the data. In all tests the beam was suspended horizontally to simulate a free-free boundary condition.

Table 2. Structural conditions.

Damage Pattern		Description
1	Undamaged	No damage (Baseline)
2	Damage 1	Cut with depth of 1 mm and 25 mm of width
3	Damage 2	Cut with depth of 2 mm and 25 mm of width
4	Damage 3	Cut with depth of 3 mm and 25 mm of width

4. RESULTS

The non-parametric transfer function Z of the structure was obtained from the power spectral density of the input/output voltages estimated by the Welch's averaged periodogram method. For illustration, figure 3 provides the real and imaginary part estimated for the healthy and damaged signals from PZT1 and the coherence function for estimative from PZT1 and PZT2. More details can be found in Silva et al. (2007). Three different ranges of frequency were analyzed. The first one from 25-45 kHz; the second one from 1-50 kHz; and the last one narrowest; from 35 to 40 kHz. For each range, the four features were computed for each PZT sensor.

The two baselines, from PZT1 and PZT2, were calculated using the mean values of the three signals in the health state. Figures 4 to 6 show a graphical view for each index considering all three tests and the four structural conditions (see table 2).

First of all, the range over 25-45 kHz seems to be more promising to detect and locate the damages. A reason for this is that the signal presented more peaks in this range (see figure 3). The other ranges were not well correlated, mainly the bigger range (see figure 5). The different number of samples to compute the features in each case can also explicate these differences. It is worth commenting that the chose of the range before performing the tests is not an obvious task and until this moment there is not a global procedure in the literature to help in this decision. The common approach is to perform a trial-error procedure considering different ranges, what can demand much time.

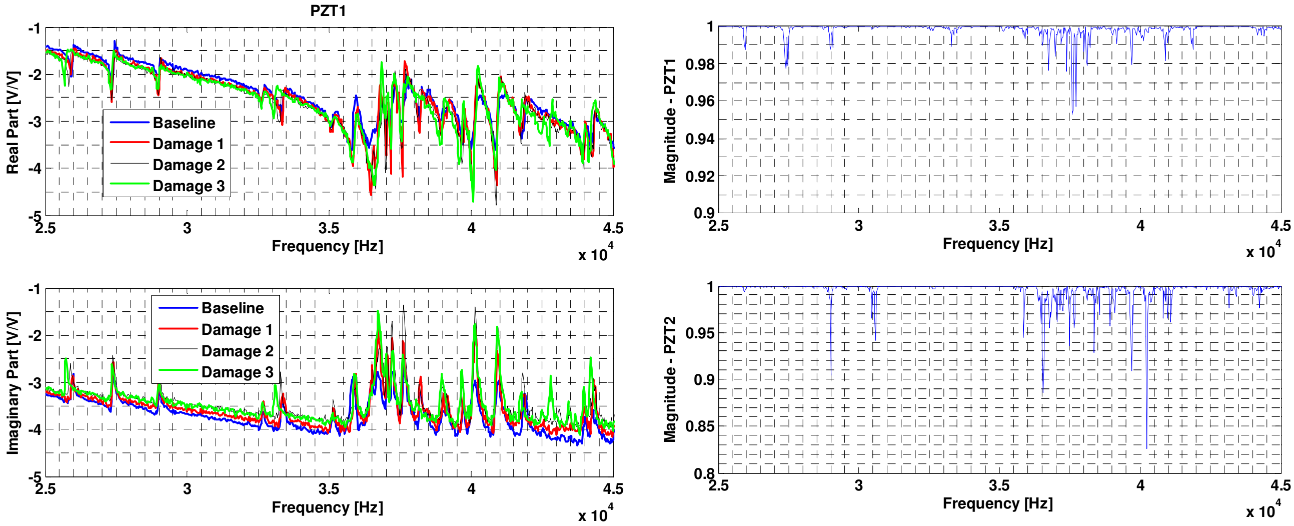

Figure 3. (a) Measurements in PZT1 for both healthy and damaged cases. (b) Magnitude squared coherence for PZT1 and PZT2 for the healthy condition.

The indexes RMSD, CCDM, H_2 and H_∞ are clearly bigger to the data from PZT1 face to data from PZT2, despite some high values from PZT2,as for instance in the figure 4b, test 1 and structural condition 2 and 4. Similar behavior can be seen and figure 5h. Note that in some figures the scales are different. However, in all cases there were indications of damage spots. The damages were introduced closer to region from PZT1. Comparing the two first features in all frequency ranges, the CCDM seems to be more trustful with smaller damage intensity, but it not present a good trend for different severities of damages. On the other hand, the H_2 norm also present a good indication for small damages and still, a better qualitative trends for variation in the damage severities, as one can be seen in the figures 4e and 4f, besides the low number of data.

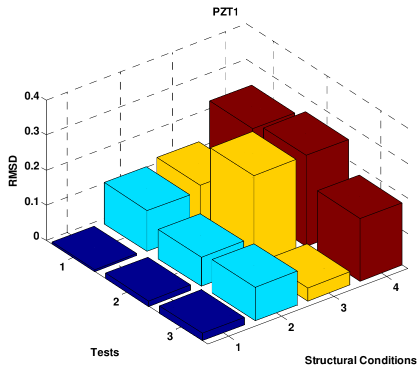

(a) RMSD – PZT1

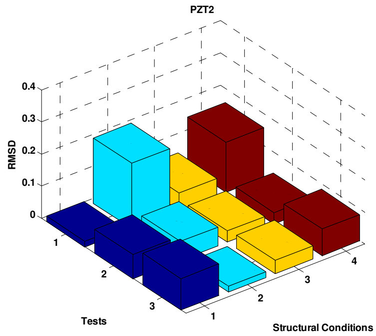

(b) RMSD – PZT2

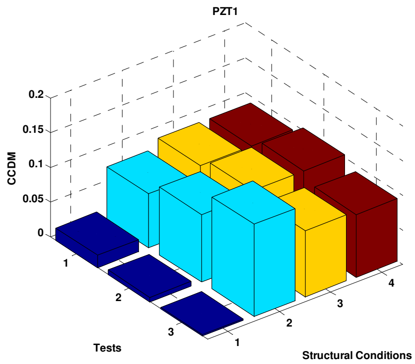

(c) CCDM – PZT1

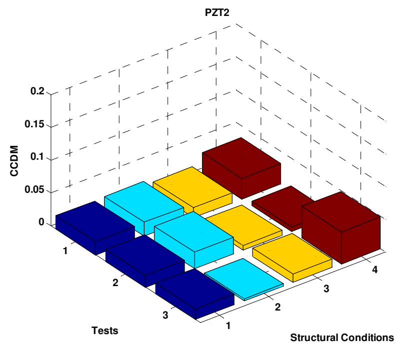

(d) CCDM – PZT2

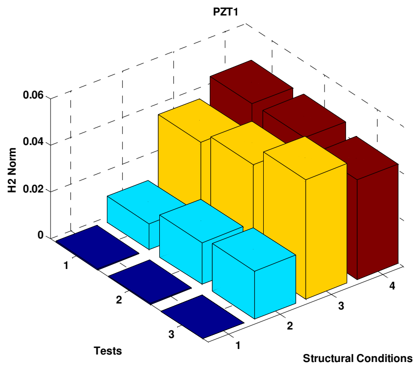

(e) H_2 norm – PZT1

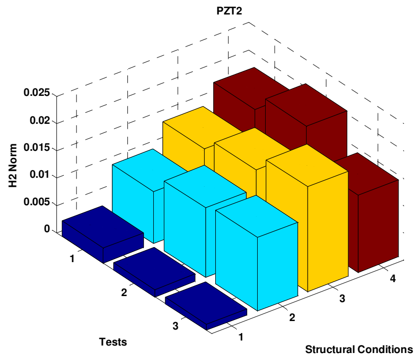

(f) H_2 norm – PZT2

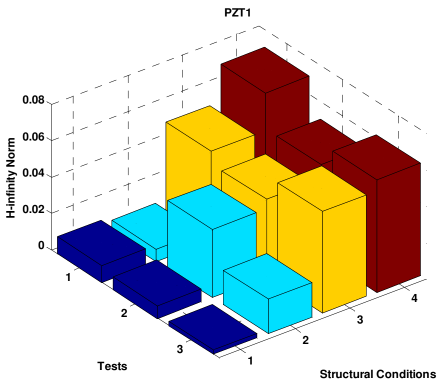

(g) H_∞ norm – PZT1

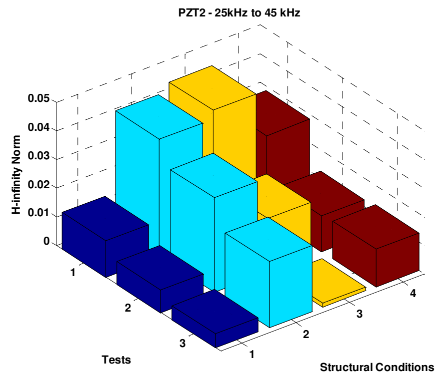

(h) H_∞ norm – PZT2

Figure 4. Comparative indexes features in the frequency range from 25 to 45 kHz.

One of the most important step to analyze the H_∞ index is to compare the peak for the same mode (or modes) before and after damage. For high frequency range is interesting to evaluate the sum of H_∞ norm from several modes to obtain more trustful information about the structural conditions.

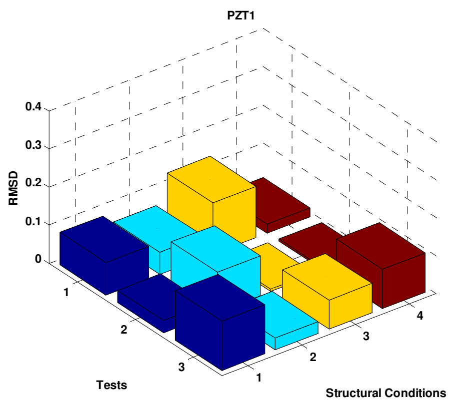

(a) RMSD – PZT1

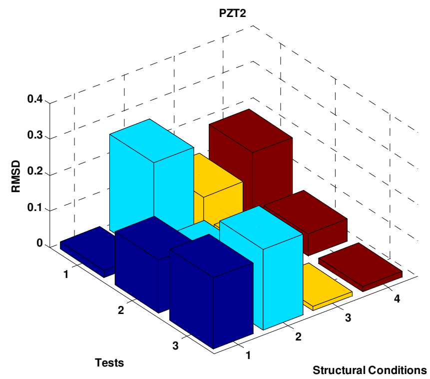

(b) RMSD – PZT2

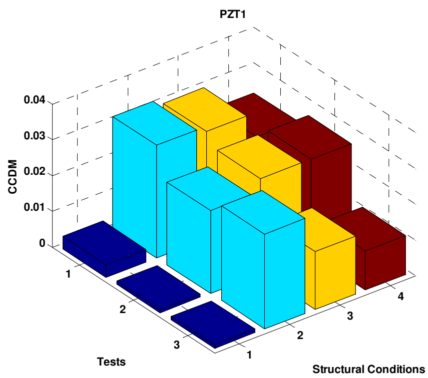

(c) CCDM – PZT1

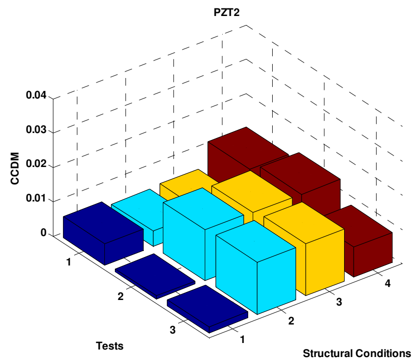

(d) CCDM – PZT2

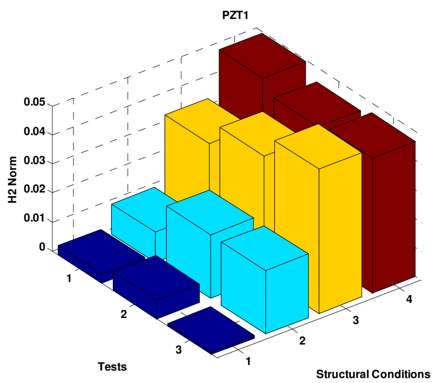

(e) H_2 norm – PZT1

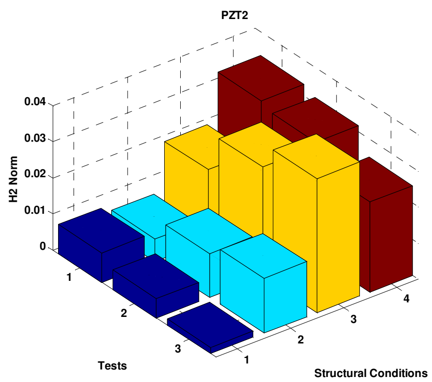

(f) H_2 norm – PZT2

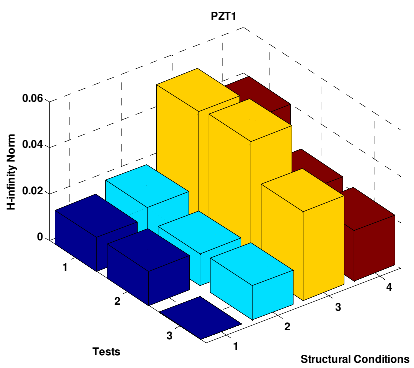

(g) H_∞ norm – PZT1

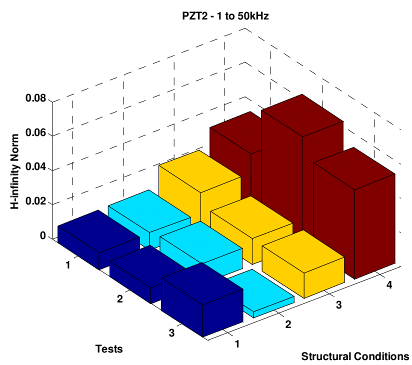

(h) H_∞ norm – PZT2

Figure 5. Comparative indexes features in the frequency range from 1 to 50 kHz.

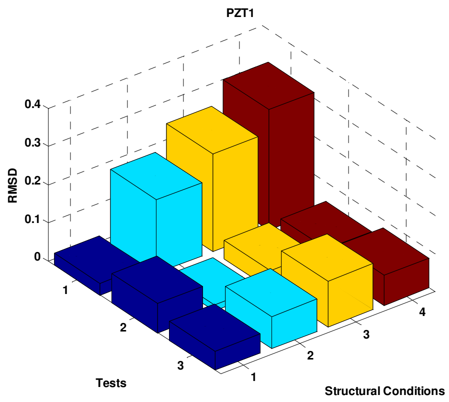

(a) RMSD – PZT1

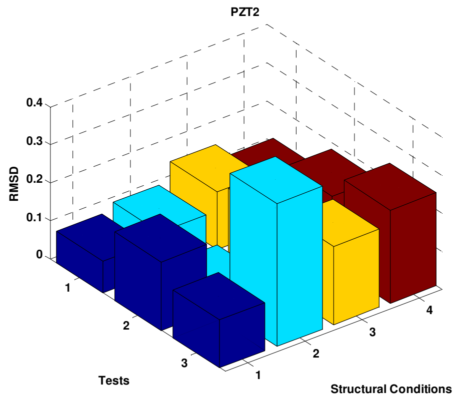

(b) RMSD – PZT2

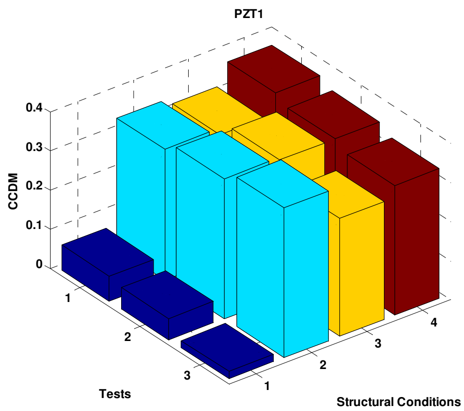

(c) CCDM – PZT1

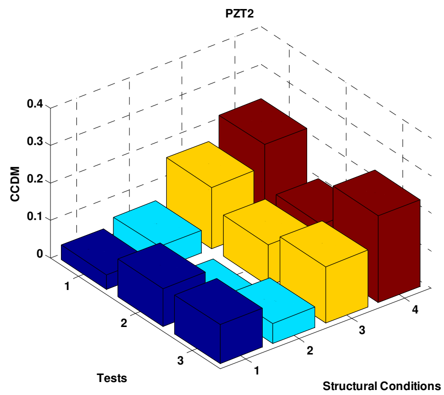

(d) CCDM – PZT2

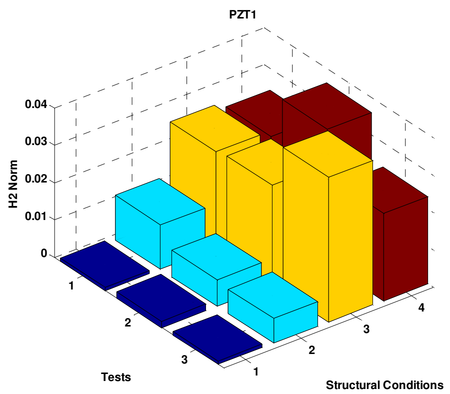

(e) H_2 norm – PZT1

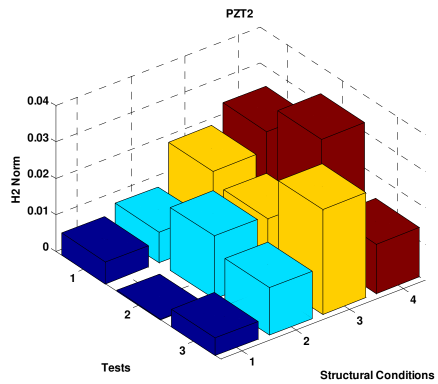

(f) H_2 norm – PZT2

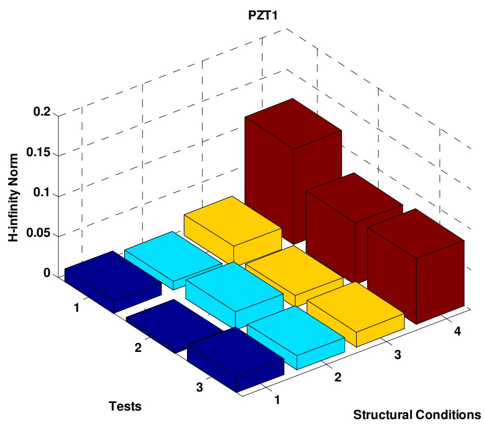

(g) H_∞ norm – PZT1

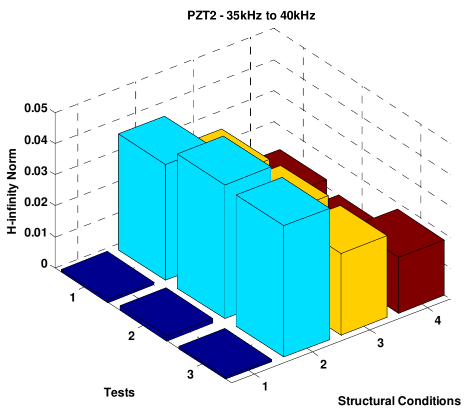

(h) H_∞ norm – PZT2

Figure 6. Comparative indexes features in the frequency range from 35 to 40 kHz.

5. FINAL REMARKS

The chose of the frequency range and the index to be applied for structural health monitoring are important issues for obtaining a success program of maintenance. This paper deals only with indexes that involve signals in frequency domain, while indexes in time domain are getting prominence in recent works. In this work, it was possible to observe that the results obtained from RMSD and CCDM indexes are similar with small prominence for the CCDM, because presented less variation in the tests. Amongst all the evaluated indexes, the one that involves the H_2 norm has shown most interesting, because it presented less variation between tests and proportional increasing of its values for each damage severity. From this paper, it is possible to conclude that the index involving the H_∞ norm can be as efficient as it one that involves the H_2 norm, however, it is important to point out that the comparison must involves peaks from the same modes for different structural conditions. Besides, when this index is computed through H_∞ norm sum of several modes for the frequency range in analysis, one can get more information about the structural condition.

6. ACKNOWLEDGEMENTS

The second author is supported by a doctorate scholarship from BIG Program/UNICAMP. The other authors are thankful to Research Foundation of the State of São Paulo (FAPESP-Brazil) for the financial support responsible for purchasing the apparatus necessary in this research and for theirs scholarships.

7. REFERENCES

Bueno, D. D., Marqui, C. R. and Lopes Jr., V., 2006, "Damage Detection in Flexible Structures Using H_2 and H_∞ norm Approaches". In: Latin American Journal of Solids and Structures – LAJSS, v. 3, pp 393-415.

Bueno, D. D., Marqui, C. R., Cordeiro, L. and Lopes Jr., V., 2006, "Optimal Placement of Sensors/Actuators in Truss Structures with Known Disturbances". In: XXIV International Modal Analysis Conference – IMAC, St. Louis, Missouri, USA.

Burl, J., B., 1999, "Linear Optimal Control: H_2 and H_∞ Methods". Addison-Wesley, ISBN 0-21-80868-4.

Gawronski, W., 1998, "Dynamics and Control of Structures, A Modal Approach", 1. Ed. New York, Springer Verlag.

Gawronski, W. K. and Juang, J. N., 1990, "Model reduction for flexible structures". In: Control and synamics systems science, ed. C.T. Leondes, v. 36, Academic Press, San Diego, CA, pp 143-222.

Gawronski, W. K. and Sawicki, J., T., 2000, "Structural Damage Detection Using Modal Norms", Journal of Sound and Vibration, pp 194-198.

Lopes Jr., V.; Park, G.; Cudney, H. H. and Inman, D. J., 2000, "Impedance based structural health monitoring with artificial neural networking". *Journal of Intelligent Material Systems and Structures*, v. 11, p. 206-214.

Mahmoud, H., Kabamba, P., T., Ulsoy, A., G. and Brusher, G., A., 2002, "Target Reduction and Balancing Using System Norms," Proceedings of ACC.

Maia, N. and Silva, J., et al., 1996, "Theoretical and Experimental Modal Analysis". Research Studies Press Ltd. Baldock, Hertfordshire, England.

Marqui, C. R., Bueno, D. D., Cordeiro, L., Silva, C. R. and Lopes Jr., V., 2006, "Experimental Damage Detection Using System Norms". In: XXIV International Modal Analysis Conference – IMAC, St. Louis, Missouri, USA.

Moura Jr., J. R. V.; Steffen Jr., V. and Inman, D. J., 2006, "Strength and damage characterization in an aircraft rib structure". *IMAC-XXIV: A Conference & Exposition on Structural Dynamics, 2006, Saint Louis - MO. IMAC-XXIV - Conference Proceedings* (CD). Bethel, CT - USA : Society for Experimental Mechanics.

Mustafa, D. and Glover, K., 1991, "Controller reduction by H_∞ balanced truncation". IEEE Transactions on automatic control, AC-36(6), 668-682.

Panossian, H.; Gawronski, W. and Ossman, J., 1998, "Balanced Shaker and Sensor Placement for Modal Testing of Large Flexible Structures". In: IMAC-XVI, Santa Barbara, CA.

Peairs, D. M; Tarazaga, P. A. and Inman, D. J., 2006, "A study on the correlation between PZT and MFC resonance peaks and damage detection frequency intervals using the impedance method". *In Proceedings of ISMA 2006, International Conference of Noise and Vibration Engineering*, Leuven, Belgium, p. 909-924.

Silva, S.; Dias Jr., M. and Lopes Jr., V., 2007, "Structural health monitoring in smart structures through time series analysis". *Submitted to Structural Health Monitoring Journal.*

Zagrai, A. N. and Giurgiutiu, V., 2001, "Electro-mechanical impedance method for crack detection in thin plates". *Journal of Intelligent Material Systems and Structures* v. 12, p. 709–718.

8. RESPONSIBILITY NOTICE

The authors are the only responsible for the printed material included in this paper.